IOP Conf. Series: Materials Science and Engineering **158** (2016) 012072 doi:10.1088/1757-899X/158/1/012072

The study of the wedge-shaped vibration-driven robot motion in a viscous fluid forced by different oscillation laws of the internal mass

A N Nuriev[1], O S Zakharova[2], O N Zaitseva[3] and A I Yunusova[4]

[1]Research Institute of Mechanics, Lobachevsky State University of Nizhnij Novgorod, Nizhnij Novgorod 603950, Russia
[2]Lobachevsky Institute of Mathematics and Mechanics, Kazan Federal University, Kazan 420008, Russia
[3]Higher Institute of Information Technologies and Information Systems, Kazan Federal University, Kazan 420008, Russia
[4]Department of Informatics and Applied Mathematics, Kazan National Technological University, Kazan 420015, Russia

nuriev_an@mail.ru

Abstract. A rectilinear motion of a two-mass system in a viscous incompressible fluid is considered. The system consists of a shell having the form of an equilateral triangular cylinder and a movable internal mass. The motion of the system as a whole is forced by longitudinal oscillations of the internal mass relative to the shell. This mechanical system simulates a vibration-driven robot, i.e. a mobile device capable to move in a resistive medium without external moving parts. Investigation of the system is carried out by a direct numerical simulation. A comparative analysis of the characteristics of the motion and flow regimes around the vibration-driven robot is carried out for different internal mass oscillation laws.

1. Introduction

Construction of vibration-driven mechanisms has long been of interest to engineers. Descriptions of numerous devices with vibrational motive power have appeared in the literature since the first half of the 20th century (see review [1]). Today the vibrational motion is a rapidly growing branch of applied mechanics and robotics.

The simplest model of a vibration-driven mechanism can be presented as a two-mass system consisting of a closed shell and movable internal mass. Devices of such architecture are often called vibration-driven robots. In a resistive medium the motion of the system as a whole is forced by longitudinal periodic oscillations of one body (internal mass) relative to another (shell). Such a principle of movement seems to be expedient for mini and micro-robots. Tightness, lack of moving external parts (screws, wheels, caterpillar tracks and etc.) are the properties, which allow using the robots for non-destructive inspections of miniature technical objects such as thin-walled pipes of small diameter, as well as in medicine, as was mentioned by several authors [2, 3].

Research of movement capabilities of vibration-driven robots were conducted earlier for medium with different resistance laws. In [4-5] the possibility of motion in an ideal fluid with related

deformations of the outer shell was considered, articles [6, 7] were devoted to the study of the movement on a rough plane in the presence of a Coulomb friction, in [8] the movement on the liquid interface was studied. Movement in the Newtonian fluid was considered in [9-14].

Despite the simple architecture, the motion control of the two-mass vibration-driven system is a non-trivial problem. The movement of such device in a viscous fluid is determined by the fluid-shell interaction, which depends on the motion law of the internal mass, the geometry of the shell and the range of Reynolds number. In this paper, we consider the problems of improving the efficiency and speed of movement due to the choice of a special law of internal mass motion of the wedge-shaped vibration-driven robot at the low Reynolds number range. For these purposes, a comparative analysis of the characteristics of the motion and flow regimes around the robot are carried out for the simple harmonic law of the internal mass motion and the special two-phase law of the internal mass motion (characterized by the alternation of fast and slow motion phases), that was obtained in [13] as the solution of energy optimization problem on the basis of a simplified model of fluid-shell interaction.

Motion simulation is carried out on the basis of the OpenFOAM software package [15]. The calculations involve both original and modified modules of the package. Calculations are carried out on high performance clusters of Kazan Federal University.

2. Formulation of the problem

2.1. Two-mass system motion

Consider a system consisting of two rigid bodies. The main body (the shell) of mass M is located in a viscous incompressible fluid, while the second body of mass m (referred to below as the "internal mass") is moving within it. The longitudinal periodic motions of the internal mass relative to the body M with which the entire system moves as a whole are investigated. The velocity of the body M will be denoted by u_M, and the displacement and velocity of the internal mass relative to the body M will be denoted by s and $v = \dot{s}$ respectively. The equations of motion of the internal mass and body M in a fixed system of coordinates have the form:

$$m(\dot{u}_M + \dot{v}) = -G,\ M\dot{u}_M = G + F \tag{1}$$

where F is the resistance of the medium to the motion of the body, G is the force of interaction of the internal mass and the body M. Eliminating the force G from (1) and normalizing the velocity u to the amplitude of internal mass oscillations U_0, the time t to RU_0^{-1}, where R is the characteristic size (length of the side of the shell) of the robot, we obtain the basic equation of motion of the two-mass system:

$$\dot{u}_M = -\mu_2\dot{v} + \mu_1\frac{R^2}{S}F \tag{2}$$

Here μ_2 is the ratio of the movable internal mass to the total mass of the robot ($\mu_2 = m/(M+m)$), μ_1 is the ratio of the mass of the viscous fluid, occupying the same volume as the robot, to the mass of the robot ($\mu_1 = M_f/(M+m)$), S is the cross-sectional area.

2.2. Fluid-structure interaction

The fluid flow around the vibration-driven robot generated by its motion is governed by the Navier-Stokes system of equations. Normalizing the spatial coordinates, time and velocity by R, RU_0^{-1}, U_0 respectively, we get the dimensionless formulation of the governing system in the following form:

$$\frac{\partial U}{\partial t} + U\cdot\nabla U = -\nabla p + \frac{1}{\mathrm{Re}}\Delta U,\ \nabla\cdot U = 0 \tag{3}$$

Where $U=(u,v)$ is the dimensionless velocity, p is the dimensionless pressure, $\mathrm{Re}=U_0R/\nu$ is the Reynolds number.

For solving this problem numerically it is convenient to rewrite governing equations in a moving (non-inertial) coordinate system associated with the shell. To retain the governing system in the form (3), we determine a new pressure as

$$p=\tilde{p}+x\dot{w}.$$

Here the first term is the pressure in the fixed coordinate system, the second term is the inertial contribution, $\dot{w}$ is the acceleration of the moving coordinate system.

On the surface of the vibration-driven robot the no-slip conditions are fulfilled:

$$u|_c=v|_c=0. \tag{4}$$

For specifying conditions at infinity we rewrite (2) in the non-inertial coordinate system. Because the acceleration in the fixed coordinate system equals the sum of the acceleration in the moving coordinate system and acceleration of the moving coordinate system, we get

$$\dot{u}|_\infty=\mu_2\dot{v}-\mu_1\frac{R^2}{S}F,\ \dot{v}|_\infty=0 \tag{5}$$

The forces acting on the vibration-driven robot by a viscous fluid in the dimensionless formulation are calculated as

$$F_p=\int_S pnds-\int_S\bar{\sigma}\cdot nds,$$

where $\bar{\sigma}$ is the viscous stress tensor, S is the surface of the robot and n is the surface normal vector. The force vector F_p can be expanded into a vertical component F_y (lift force) and a horizontal component F_x, which consists of the drag force and inertia force. The inertial force acting on the cylinder due to the fluid acceleration can be split into two parts: the inertia force of added mass, arising due to the local acceleration near the cylinder, and the Froude-Krylov force, which is related to the pressure gradient created in the fluid by the flow oscillations. The Froude-Krylov force for the considered case can be calculated as

$$F_{fk}=\int_S x\dot{w}nds. \tag{6}$$

Taking into account (6), the infinity boundary condition (5) can be rewritten

$$\dot{u}|_\infty=\mu_2\dot{v}-\mu_1\frac{R^2}{S}(F_x-F_{fk}) \tag{7}$$

The system of equations (3), (4) and (7) completely describes the motion of vibration-driven robot of arbitrary shape in a viscous fluid for a given law of the internal mass motion.

3. Numerical model

3.1. Spatial and time discretization

The numerical solution is carried out using the OpenFOAM software package. The computational domain is constructed as a rectangular parallelepiped measuring 50×30×1 with an equilateral triangular cylinder in the center of it. For modelling the plane flow a three-dimensional domain is used in accordance with the software features. In chosen Cartesian coordinate system the edges of the parallelepiped are parallel to the main axes, and the plane of flow is parallel to the plane *xOy*.

For the discretization of the computational domain we use block-structured grids, generated by blockMesh utility of OpenFOAM. Each grid block is decomposed into disjoint hexahedral cells. The decomposition in the z-axis direction consists of one cell, which causes the flow in this direction not to be calculated due to the two-dimensional problem formulation.

The discretization of the equations of fluid flow in the OpenFOAM package is carried out by the finite volume method (FVM) in the Cartesian coordinate system. The discrete values of the velocity

and pressure are localized in the cell centers of the computational grids. To calculate the volume integrals over the control volume the general Gauss procedure is used. For the approximation of the pressure gradient the linear interpolation is applied. To interpolate the variables in convective terms nonlinear NVD (normalized variable diagram) scheme "Gamma" is used. In the diffusion terms, when the discretization of the Laplace operator is carried out, the normal velocity gradients on the surface of the cells are approximated by using a symmetric second-order scheme with non-orthogonality correction (for more details see [16, 17]).

The implicit Euler scheme is used for the time discretization of the system of equations. The time step for all calculations is chosen from the condition, that the maximum Courant number does not exceed 0.1.

3.2. Iteration scheme

The resulting discrete problem solution is based on the PISO method implemented in the icoFoam solver of OpenFOAM. At each time iteration of the algorithm additional steps for updating the boundary conditions (9) are defined. Updating is implemented by the deferred correction scheme. The resulting iterative scheme for calculating the values of unknowns on the j-th time layer can be represented as follows:

1. The predictor for the acceleration of the moving coordinate system is calculated as

$$\dot{w}_p^j = 2\dot{w}^{j-1} - \dot{w}^{j-2}.$$

2. The boundary conditions at the input and output boundaries are updated according to (9), where the acceleration is calculated as the sum of the predictor and corrector for the old time layer, and the velocity is determined by the 2nd order upwind difference scheme:

$$\dot{u}_\infty^j = -\dot{w}_p^j + \dot{w}_c^{j-1},\ u_\infty^j = (-2\dot{u}_\infty^j dt + 4u_\infty^{j-1} - u_\infty^{j-2})/3$$

3. The discrete governing system of the fluid motion is solved by the PISO method, the force F_x is calculated.

4. The real acceleration of the system is calculated using the new value of the force:

$$\dot{w}^j = -\mu_2 \dot{v}^j + \mu_1 \frac{R^2}{S} F^j$$

5. The corrector is calculated as

$$\dot{w}_c^j = \dot{w}_p^j - \dot{w}^j.$$

We used 5 pressure correction steps in the PISO method. To solve the system of equations for the pressure, the preconditioned conjugate gradient (PCG) method with the geometric-algebraic multigrid (GAMG) preconditioner was applied. In the GAMG realization we used the Gauss-Seidel method with one and two pre- and postrelaxations for smoothing, respectively, and the faceAreaPair algorithm for agglomeration of the mesh cells. The systems of equations for the velocity components were solved by the bi-conjugate gradients (PBiCG) method with the preconditioner based on an incomplete LU factorization. All calculations were distributed according to the MPI technology and the method of decomposition of the calculation domain.

4. Results of numerical experiments

The numerical simulation was performed for the simple harmonic and the special two-phase laws of the internal mass motion (see fig. 1). Calculations were carried out in the range of Reynolds numbers $50 < \mathrm{Re} < 250$ for the following combination of control parameters: $\mu_1 = 0.06$, $\mu_2 = 0.61$, $A = H$, where $H = \sqrt{0.75}$ is the height of the triangle. Calculations were started from different initial approximations determined by different initial flow velocities. To examine the stability of motion regimes, external disturbances were included into the flow by the Martinez method [18].

The next main characteristics of the motion were considered: the average speed U_a and the motion efficiency coefficient η [19], which defines the energy consumption due to the body motion by means

of an internal motive power. Using angular brackets to denote the average for a period of motion, we define them as follows:

$$U_a = < U >,\ \eta = \frac{N_0}{N_{vbr}}$$

Here $N_0 = N(< U >)$ is the minimum power required for the body motion with velocity U_a (the values of N_0 for different values of the parameter Re are obtained according to auxiliary calculations), $N_{vbr} = N(U)$ is the power expended on the motion of the robot with a fixed average velocity of U_a.

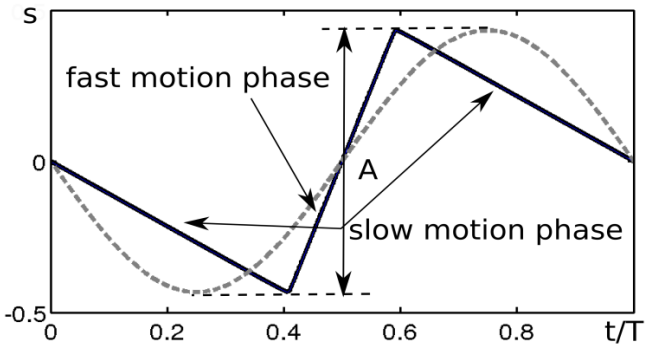

Figure 1. Harmonic (dashed line) and two-phase (solid line) laws of the internal mass motion

4.1. Harmonic law of the internal mass motion

For the harmonic law of the internal mass motion the difference between the forces on a direct and return phases of the movement, acting on the shell, causes the non zero average velocity of the whole system is achieved by asymmetrical flow around the shell with respect to the half-period.

Evolution of the motion characteristics depending on the Reynolds number for different regimes is shown in fig. 2 and fig. 3.

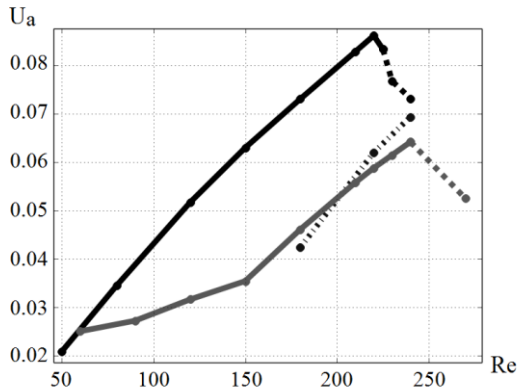

Figure 2. Average velocity of movement. Different curves represent different flow regimes: solid gray - H1, dashed gray –H2, doted – H2, solid black - TP1, dashed black - TP2.

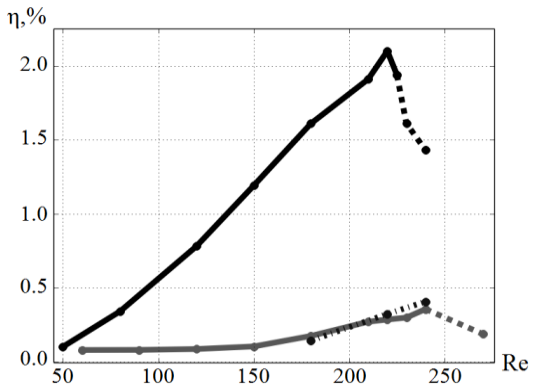

Figure 3. Efficiency of movement. Different curves represent different flow regimes: solid gray - H1, dashed gray –H2, doted – H2, solid black - TP1, dashed black - TP2.

In the area of small Reynolds numbers (Re < 170) a unique, periodic and symmetric with respect to the oscillations axis regime H1 is realized (see fig. 4). This regime corresponds to the vertex forward motion of the triangular robot. The growth of flow complexity and non-linear effects in this area lead to increase of the values of average velocity and efficiency coefficient. When Re becomes larger than

170, simultaneously with the basic regime H1 another periodic and symmetric with respect to the oscillations axis motion regime H2 appears, that implements oppositely directed base forward movement (the flow pattern is presented in fig. 4). Thus a hysteresis of motion regimes arises. Switching to one of these regimes depends on the initial parameters of the robot motion. The values of average velocity and efficiency of movement of the robot in regime H2 approximately the same as for regime S.

In the neighbourhood of Re = 240 the basic regime H1 transforms to a quasiperiodic asymmetrical regime H3 (see fig. 4). The transformation is associated with the crisis of the basic parameters of motion that is particularly noticeable on the graphs of the efficiency coefficient and average velocity (see fig. 2, 3).

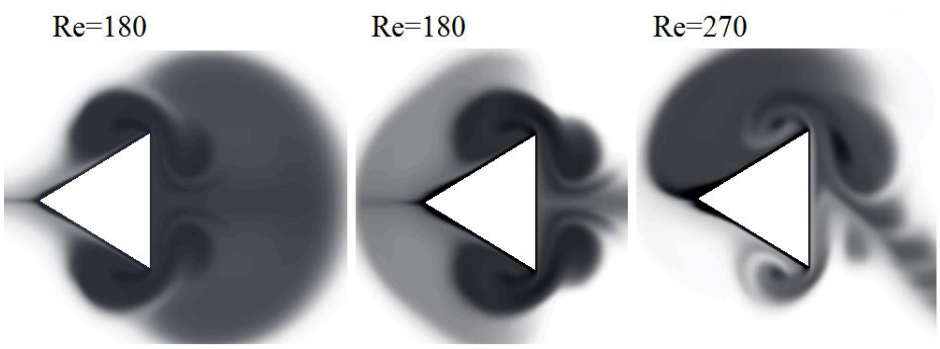

Figure 4. Flow patterns around vibration-driven robot at different motion regimes for harmonic oscillations of the internal mass. H2 (left), H1 (central), H3 (right).

4.2. Two-phase law of the internal mass motion

The structure of the considered two-phase law is shown in fig. 1. As can be seen the full period of the movement consists of two main phases: a long phase of slow motion and a short phase of fast motion, during which the internal mass moves with constant velocity. The transition between these phases is realized in a short time interval, the duration of which is less than 2% from the full period of movement. The main idea of this law is that during the slow long phase the shell of vibrating-driven robot should experience less resistance than on the fast return phase, when due to the nonlinear dependence of the resistance on the speed the forces opposing the movement of the robot increase significantly. To improve the efficiency of movement the long phase is combined with the vertex forward motion of the shell.

The two-phase motion law of the internal mass provides the only one possible direction of motion of the system (in the considered case it is vertex forward motion). In the area of small Reynolds numbers (Re < 220) a unique, periodic and symmetric with respect to the oscillations axis regime TP1 is realized (see fig. 5). In the neighbourhood of Re = 220 it transforms to a quasiperiodic asymmetrical regime TP2 (see fig. 5).

Comparison of the simulation results for different laws of the internal mass motion (see fig. 2,3) shows that the two-phase law provides a higher speed of movement (up to 50%) in the fluid, and is significantly more efficient (up to 4 times) in terms of energy consumption.

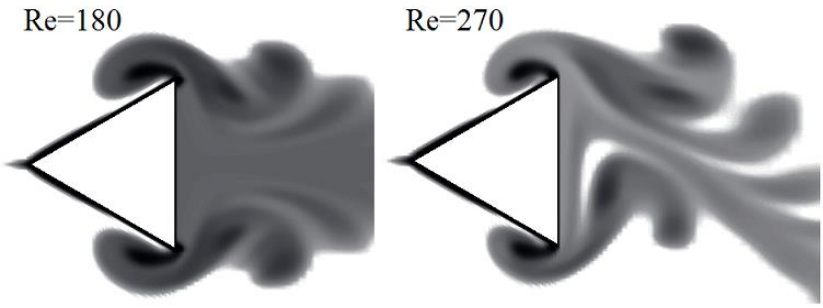

Figure 5. Flow patterns around vibration-driven robot at different motion regimes for two-phase oscillation law of the internal mass. TP1 (left), TP2 (right).

Acknowledgments
The reported study was partially supported by RSF, research project No. 15-19-10039. Numerical model was designed in the Lobachevsky State University of Nizhnij Novgorod.

References
[1] Gulia N V 1982 Inertia (Moscow: Nauka) (in Russian).
[2] Chernous'ko F L 2008 The optimal periodic motions of a two-mass system in a resistant medium *J. Appl. Math. Mech.* **72** pp. 116-125.
[3] Bolotnik N N, Figurina T Y and Chernous'ko F L 2012 Optimal control of the rectilinear motion of a two-body system in a resistive medium *J. Appl. Math. Mech.* **76** pp. 1-14.
[4] Lighthill M J 1952 On the Squirming Motion of Nearly Spherical Deformable Bodies through Liquids at Very Small Reynolds Numbers *Comm. Pure Appl. Math*. **5 (2)** pp. 109–118
[5] Saffman P G 1967 The Self-Propulsion of a Deformable Body in a Perfect Fluid *J. Fluid Mech.* **28 (2)** pp. 385–389.
[6] Ramodanov S M, Tenenev V A and Treschev D V 2012 Self-propulsion of a Body with Rigid Surface and Variable Coefficient of Lift in a Perfect Fluid *Regul. Chaotic Dyn.* **17(6)** pp. 547–558.
[7] Chernous'ko F L 2005, On the motion of a body containing a movable internal mass *Dokl. Phys.* **50** pp. 593-597.
[8] Chernous'ko F L 2006 Analysis and optimization of the motion of a body controlled by means of a movable internal mass *J. Appl. Math. Mech.* **70** pp. 819-842.
[9] Volkova L Yu and Jatsun S F 2011 Control of the Three-Mass Robot Moving in the Liquid Environment *Rus. J. Nonlin. Dyn.* **7(4)** pp. 845–857.
[10] Childress S, Spagnolie S E and Tokieda T A 2011 Bug on a Raft: Recoil Locomotion in a Viscous Fluid *J. Fluid Mech.* **669** pp. 527–556.
[11] Auziņš J, Beresņevičs V, Kaktabulis I and Kuļikovskis G. 2011 Dynamics of Water Vehicle with Internal Vibrating Gyrodrive. *Vibration Problems ICOVP 2011. Supplement: The 10th International Conference on Vibration Problems*, Czech Republic, Prague, 5-8 September.
[12] Vetchanin E 2013 The Self-propulsion of a Body with Moving Internal Masses in a Viscous Fluid *Regular and Chaotic Dynamics* **18** pp. 100–117.
[13] Egorov A G, Zakharova O S 2010 The energyoptimal motion of a vibrationdriven robot in a resistive medium *J. Appl. Math. Mech.* **74** p. 443.
[14] Egorov A G, Zakharova O S 2012 Optimal quasistationar motion of vibrationdriven robot in a viscous liquid *Izv. Vyssh. Uchebn. Zaved.* **2** pp. 57–64.
[15] Open foam (the open source cfd toolbox): User guide version 2.2.1, URL: http://www.openfoam.org/docs/user/.
[16] Nuriev A N and Zaytseva O N 2013 Solution to the problem of oscillatory motion of a cylinder in a viscous fluid in the OpenFOAM package *Heald of Kazan Technological University* **8** pp.

116-123.

[17] Egorov A G, Kamalutdinov A M, Nuriev A N and Paimushin V N 2014 Theoretical-experimental method for determining the parameters of damping based on the study of damped flexural vibrations of test specimens. 2. Aerodynamic Component of Damping *Mech. Compos. Mater.* **50** pp. 267-275.

[18] Martinez G 1979 Caractristiques dynamiques et thermiques de l'coulement autour d'un cylindre circulaire a nombres de reynolds moderes, Ph.D. thesis, I.N.P. Toulouse.

[19] Maertens A P, Triantafyllou M S and Yue D K P 2015 Efficiency of fish propulsion *Bioinspiration & Biomimetics* **10(4)**